

Dielectric and electromechanical characterisation of fine-grain $\text{BaTi}_{0.95}\text{Sn}_{0.05}\text{O}_3$ ceramics sintered from glycolate-precursor powder

Ludwig Geske, Volker Lorenz, Thomas Müller, Lothar Jäger, Horst Beige, Hans-Peter Abicht, Volkmar Mueller

Fachbereich Physik, Martin-Luther-Universität Halle, F.-Bach-Platz 6, D-06108 Halle, Germany

Fachbereich Chemie, Martin-Luther-Universität Halle, Kurt-Mothes-Str.2, D-06120 Halle, Germany

Abstract

Nanocrystalline $\text{BaTi}_{0.95}\text{Sn}_{0.05}\text{O}_3$ (BTS-5) powder was synthesised from glycolate-precursors, and used to sinter fine-grain BTS-5 ceramics. We compare sintering behaviour, microstructure as well as dielectric and electromechanical properties of the advanced ceramics with ceramics sintered from classical mixed oxide powder.

Keywords: Precursor complex, Grain size, Piezoelectric properties, Ferroelectric properties, BaTiO_3 and titanates

1. Introduction

The strong temperature dependence of macroscopic properties limits the applicability of most ferroelectrics with sharp phase transition in technical devices. The performance of disordered ferroelectrics is usually higher, due to the smeared dielectric anomaly accompanying its

diffuse phase transition.¹ In $\text{BaTi}_{1-x}\text{Sn}_x\text{O}_3$ (BTS-100x) ceramics for example, the isovalent Sn-substitution on Ti-sites makes it possible to reduce the temperature dependence and to control the room temperature values of dielectric, electromechanical and elastic coefficients in a fairly wide range.¹⁻⁶ With increasing Sn-content, the temperature T_c of the paraelectric-ferroelectric phase transition decreases considerably. In addition, the phase transition of BTS becomes increasingly diffuse,¹ as displayed by significant deviations from the Curie-Weiss-law of the temperature dependent permittivity reported for $x > 0.05$.² Below the permittivity maximum temperature T_m , the ferroelectric domain-structure was observed for $x \leq 0.13$, confirming ferroelectric long-range order in this composition range.³ The analysis of temperature dependent permittivity data taken at various frequencies revealed characteristic features of relaxor ferroelectrics for $x \geq 0.2$.^{2,4} Recent electromechanical studies^{5,6} demonstrated that BTS is basically suitable as environmental-friendly material for electromechanical sensor and actuator applications.⁷

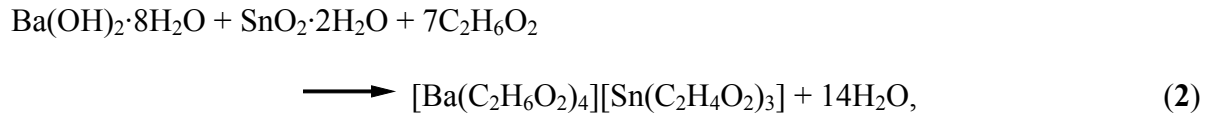
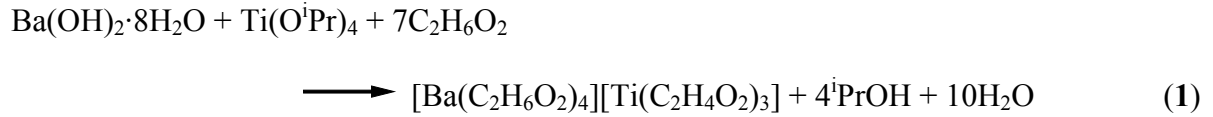
Beside the variation of the chemical composition, the reduction of grain size represents another tool widely used to improve the temperature stability of macroscopic properties in ferroelectric ceramics. Moreover, fine-grain piezoelectric ceramics have been shown to possess improved machinability, increased mechanical strength and higher reliability.⁸ This allows to design miniaturised devices operating at low driving voltages. Numerous work has been done to elucidate the influence of grain size on the dielectric^{9,10} and piezoelectric¹¹ properties, the domain structure,^{10,12} the tetragonal lattice distortion¹³ and the Curie-temperature¹³ of barium titanate ceramics. In BTS-10 corresponding to the diffuse phase transition state of BTS, the electromechanical strain inducible in large electric fields was shown to be less temperature dependent in the fine-grain ceramics.⁵

Fine powders with uniform grain sizes are required to obtain fine-grain ceramics. In contrast to barium titanate, where several chemical techniques such as sol-gel,¹⁴ modified

Pechini processes¹⁵ and precipitation methods¹⁶ have been developed to fabricate ultra-fine powders, most data available for BTS focus on ceramics sintered from conventional powders, obtained from solid state reaction of BaCO₃ with TiO₂, SnO₂ or mixtures of both oxides. Thermolysis reactions of coordination compounds, although more complex in nature, offer clear advantages for the synthesis of ultra-fine powders at relatively low temperatures. In particular, the stoichiometric ratio between barium and titanium ions can be controlled on a molecular basis. In this study, we used fine powder synthesised from barium titanium/tin glycolate-precursors to sinter fine-grain BTS ceramic. We present results illustrating the influence of microstructure and powder processing onto the electromechanical response of BTS both in small and large electric fields. The experiments were carried out on BTS-5, which composition displays a sharp ferroelectric phase transition, as far as conventional coarse-grain ceramics are concerned. We compare the properties of the fine-grain BTS-5 ceramic with those of coarse-grain ceramics sintered from conventional mixed oxide powder.

2. Experimental

Conventional BT-powder was synthesised by solid state reaction of BaCO₃ (Saded VL 600) and TiO₂ (Merck 808). In order to obtain BTS, BaCO₃ and SnO₂ (Merck 7818) were added in a second calcination step ($t_{ca}=2h$ at $T_{ca}=1375K$). Thermolysis reactions of ionic barium-titanium and barium-tin complexes were used to obtain phase pure BTS powders with fine and uniform grain size. The method chosen allows similar reaction conditions for the synthesis of the titanium and tin compounds, respectively, and leads to homologous derivatives for both elements. First we modified the reaction described by *Day et al.*¹⁷ which was recently used to synthesise $[Ba(C_2H_6O_2)_4(H_2O)][Ti(C_2H_4O_2)_3]$. According to the equations



we obtained $[\text{Ba}(\text{C}_2\text{H}_6\text{O}_2)_4][\text{Ti}(\text{C}_2\text{H}_4\text{O}_2)_3]^{18}$ (BTG) and the homologous $[\text{Ba}(\text{C}_2\text{H}_6\text{O}_2)_4][\text{Sn}(\text{C}_2\text{H}_4\text{O}_2)_3]^{19}$ (BSG). Crystal structure analyses revealed that BTG and BSG crystallise isotypically (space group R3c). Corresponding amounts of both compounds were dissolved in ethyleneglykol and co-crystallised. As confirmed by XRD, this results in two types of BTSG mixed crystals which are either rich in Ti, or rich in Sn. Upon heating, the solvate molecules are eliminated at 220 °C and $\text{Ba}[\text{Ti}_{1-x}\text{Sn}_x(\text{C}_2\text{H}_4\text{O}_2)_3]$ is formed. After annealing at 1000 °C for 2 hours, we obtained BTS-5 powder with rather uniform globular grains (average diameter 400nm).

From the fine-milled powders, green bodies were pressed to a density $\rho=3.1\text{g/cm}^3$, and sintered in air for 1h at 1400°C (heating TMA92 rate 10K/min). The shrinking of the pellets upon sintering was examined with a dilatometer (Setaram Inc.) After sintering, samples were polished and chemically etched to investigate the ceramic microstructure by environmental scanning microscopy (ESEM) and optical microscopy, respectively.

The dielectric characterisation was carried out on bar-shaped samples, whose large faces were evaporated with Al-electrodes. The small signal permittivity $\epsilon=\epsilon'-ie''$ was measured with a HP4192A impedance analyser. The sample geometry chosen ($l \times w \times t=20.0 \times 2.2 \times 0.72\text{mm}^3$ for the coarse-grain and $13.3 \times 1.9 \times 0.48\text{mm}^3$ for the fine-grain ceramic) assured isolated length vibration of the poled sample, if the frequency of the AC-measuring field ($E_{ac}=0.017\text{V/mm}$) approached the mechanical resonance frequency f_r . The dielectric resonance spectrum of the sample, contacted with thin Cu-wires positioned at the

vibration node, carries information about the electromechanical coupling factor $k_{31}=d_{31}^2/(\epsilon_0\epsilon_{33}^T s_{11}^E)$, and the elastic and piezoelectric coefficients s_{11}^E and d_{31} . It was least-squares fitted to the theoretical expression

$$Y = i \left[\frac{lw}{t} \left(\epsilon - \frac{d_{31}^2}{s_{11}^E} \right) \omega + \frac{2w}{t\sqrt{\rho}} \frac{d_{31}^2}{(s_{11}^E)^{\frac{3}{2}}} \tan \left(\frac{1}{2} l \sqrt{s_{11}^E \rho} \omega \right) \right] \quad (3)$$

for the length extensional vibration of a piezoelectric resonator.²⁰ From the complex coefficient s_{11}^E and d_{31} , we additionally obtained information about the elastic and electromechanical losses in BTS-5.

The AC-electric field $E_{ac}=E_m \sin\omega t$ ($E_m=2\text{kV/mm}$, $\omega/2\pi=0.1\dots 200\text{Hz}$), generated by a high voltage amplifier Trek609E-6, was applied in order to investigate the dielectric and electromechanical large field response of BTS-5. P(E)-hysteresis loops were recorded with a home made Miller-integrator, whose output voltage was analysed using a 12-bit PC-data acquisition board DT3010 (Data Translation Inc.). "Butterfly" strain-field-loops S(E) were measured with a capacitive dilatometer described elsewhere.²¹

3. Results

3.1. Sintering behaviour and microstructure

Sintering of the conventional and of the glycolate-precursor powder lead to BTS-5 ceramics with significantly different microstructures. Despite the fairly narrow grain size distribution of the glycolate-precursor powder, we sintered ceramics with rather inhomogeneous grain sizes. ESEM images (see Fig. 1) show few larger grains ($\leq 5\mu\text{m}$) within a matrix of smaller grains ($< 2\mu\text{m}$). For the same sinter regime, we obtained from the conventional mixed oxide

powder ceramics with an average grain size of $60\mu\text{m}$, containing some large grains with up to $150\mu\text{m}$ size. Due to the different grain sizes of the ceramics examined, we refer in what follows to the glycolate-precursor ceramic as fine-grain BTS-5, in contrast to the coarse-grain BTS-5 obtained from the conventional mixed oxide powder.

Densities of 5.4g/cm^3 and 5.7g/cm^3 were determined for the fine-grain and coarse-grain ceramic, respectively. The reduction of the sintering temperature to 1350°C lead to incomplete densification of the glycolate-precursor pellet. Although the differences between both batches with respect to the final density, accomplished after 1h at $T_s=1400^\circ\text{C}$, are rather small, the shrinking behaviour during the sintering time differs significantly (Fig. 2). The shrinking curve of the mixed oxide pellet shows two distinct maxima. The high temperature maximum, corresponding to the eutectic temperature of the system BaO/TiO_2 , is not observed upon sintering of the glycolate-precursor pellet, which is characterised by a single broad maximum.

The different sintering behaviour of both batches should be discussed in terms of the different mixing agents used during fine-milling. The conventional powder was fine-milled in water, which is known to solve BaO .²² Due to the Ti-excess thus established in the fine-milled powder, liquid phase forms upon sintering at 1330°C , leading to accelerated grain growth. As the glycolate precursor powder was fine-milled in isopropanol, the stoichiometric Ba:Ti ratio was maintained.

3.2. Dielectric characterisation

Temperature scans were carried out to investigate the complex permittivity in the vicinity of the temperature T_c of the paraelectric-ferroelectric phase transition. As shown in Fig. 3, the dielectric anomaly of the BTS-5 sample sintered from glycolate-precursors displays charac-

teristic features of fine-grain barium titanate ceramics.⁹ The peak height at T_c amounts to only 45% of the conventional mixed oxide sample. In addition, the phase transition of the fine-grain ceramic is considerably diffuse, as the peak width increases by a factor of two, and the peak becomes more symmetric. In barium titanate, the gradual smearing of the dielectric anomaly with decreasing grain size was explained in terms of a local distribution of Curie-temperatures, which arises due to internal stress within the grains, rather than due to chemical inhomogeneity.⁹ The maximum permittivity temperature T_m , on the other hand, does not differ significantly between both samples. This temperature decreases steeply ($dT_m/dx \approx 800K$) with Sn-content x .¹ As the grain sizes of the ceramics examined are large enough so that the decrease of the transition temperature, observed in $BaTiO_3$ for very small particle size,²³ should be neglected, we conclude that the Sn-content established during powder processing was nearly the same.

The permittivity of the coarse-grain BTS-5 ceramic exceeds those of the fine-grain ceramic in the whole paraelectric phase. In the ferroelectric phase, however, the bigger permittivity values are observed for the fine-grain ceramic. This holds for the tetragonal ferroelectric phase of BTS-5, as well as for temperatures below the temperature $T_2 \approx 307K$ of the tetragonal-orthorhombic phase transition, which manifests as a shoulder in the $\epsilon'(T)$ -curve. The grain size dependent dielectric properties in the ferroelectric phase of $BaTiO_3$ ceramics were explained in terms of the dielectric domain-wall contribution.¹² Enhanced dielectric response was observed for grain sizes $0.5..2\mu m$, for which the domain-wall density (i.e., the total wall area per volume) is biggest. Further indication for relevant domain-wall contributions in our fine-grain BTS-5 ceramic provides the pronounced low-frequency dispersion below T_c , which is clearly stronger than in the coarse-grain sample. The domain-wall response of the glycolate-precursor ceramic may be further increased due to its higher chemical purity, leading to smaller pinning and higher mobility of the domain-walls.

The ferroelectric phase transition is accompanied by a peak of the imaginary part ϵ'' , whose height depends on measuring frequency (Fig. 3b). The $\epsilon''(T)$ -peak depends also strongly on microstructure, as the anomaly is much less pronounced in the fine-grain ceramic. Due to the loss accompanying the dielectric domain-wall contribution, the bigger ϵ'' values in the ferroelectric phase are observed for the fine-grain ceramic. In the paraelectric phase, ϵ'' starts to increase again at elevated temperatures. This is related both to the temperature increase of the conductivity, and to dielectric low-frequency dispersion, which manifests in the $\epsilon'(T)$ curve of the fine-grain ceramic above 130°C (see Fig. 2a). In coarse-grain BTS-5, the dielectric loss in the paraelectric phase is considerably smaller, and the low-frequency dispersion $\epsilon'(f)$ becomes discernible only at $T > 205^\circ\text{C}$ (data not included in Fig. 2a). The strong relationship between microstructure and dielectric loss points to the crucial role of the grain boundaries for the high temperature dielectric properties at elevated temperatures. Apparently the dielectric contribution of charges localised at the grain boundary causes the low-frequency dispersion, which is much more pronounced in the fine-grain ceramic due to the considerably bigger total grain surface.

BTS-5 examined in this study belongs to BTS-compositions with long-range ordered ferroelectric phase, where the polarisation reversal in large electric fields proceeds by ferroelectric switching (i.e. processes of domain-nucleation and -growth), which manifests in the hysteresis loop $P(E)$. As it can be seen from the data plotted in Fig. 4, the ferroelectric hysteresis loop of BTS-5 does not show a true saturation branch. If the maximum polarisation P_{max} is obtained at E_{max} and the electric field decreases again, pronounced "backswitching" (i.e. P decreases before the negative coercive field $-E_c$ is reached) leads to a rather small remnant polarisation P_{rem} , which amounts only to 50% of P_{max} . (Both parameters P_{max} and P_{rem} increase slightly if the frequency of the sinusoidal field is reduced.) The hysteresis loops of the coarse-grain and fine-grain ceramic are similar, but quantitative differences are obvious:

As compared to coarse-grain BTS-5, the coercive field of the fine-grain ceramic is 40% bigger and P_{rem} and P_{max} are approximately 25% smaller.

3.3. Electromechanical properties

The remnant polarisation induced during the $P(E)$ measurements in the orthorhombic phase of BTS-5 was sufficient to excite piezoelectric length vibrations of the samples subjected to the small AC-measuring field ($E_{\text{ac}}=0.017$ V/mm). In Fig. 5, real and imaginary part of the admittance are shown in the vicinity of the mechanical resonance frequency. Clearly, the frequency dependence $Y(\omega)$ can well be approximated by eq.(3). The elastic coefficient $s_{11}^E=s_{11}^{E'}-s_{11}^{E''}$, the piezoelectric coefficient $d_{31}=d_{31}'-d_{31}''$, the mechanical quality $Q=s_{11}^{E'}/s_{11}^{E''}$ and the coupling factor K_{31} , determined from least square fits of the data, are given in table 1.

The piezoelectric coupling factor of the poled coarse-grain ceramic is rather small, as compared to values reported for lead zirconate titanate (PZT) piezoceramics,²⁴ and is even smaller in fine-grain BTS-5. This seems to be mainly due to the small remnant polarisation of our samples (see Fig. 4). According to results reported for BTS-10,⁵ considerably bigger piezoelectric coefficients should be expected for the DC-biased sample. Interestingly, the imaginary part K'' of the coupling factor is non-zero, as it was recently also observed in soft and hard PZT's.²⁵ We find the bigger ratio $K''/K' \approx 0.013$ in the fine-grain ceramic (coarse-grain BTS-5: $K''/K' = 0.0075$).

The microstructure also influences significantly the elastic properties. The fine-grain ceramic is considerably softer, and its mechanical quality decreases by nearly 50%. As the motion of non-180° domain-walls contributes to the elastic coefficient, this provides another indication for increased domain-wall activity in the fine-grain ceramic. However, we find that $s_{11}^{E'}$ decreases with the electric field applied during poling of the sample. Therefore, the

different $s_{11}^{E'}$ values may also point to differences with respect to the poling level established in the samples.

Strain-field curves $S_3(E_3)$, characterising the electromechanical response in large electric fields, are shown in Fig 6. The data were taken after several cycles of the sinusoidal field ($f=10$ Hz). As it can also be seen from the results of our piezoelectric resonance investigations, the grain size crucially influences the electromechanical properties of BTS-5: The maximum strain $S_{3\max}=S_3(E_{\max})$ inducible at $E_{\max}=2\text{kV/mm}$ in the fine-grain ceramic is about 15% smaller than in coarse-grain BTS-5. However, taking into account previous results obtained for BTS-10,⁵ it may be expected that the detrimental reduction of $S_{3\max}$ is at least partially compensated by the advantage of the reduced temperature dependence $S_{3\max}(T)$ in fine-grain ceramics. In BTS-10 and BTS-13, strain-field curves were reported which display remarkable linear regions and are nearly hysteresis-free.⁵ These compositions belong to the diffuse phase transition state of BTS, where both relaxor-like and domain-switching contributions are relevant.⁶ Similar to the result of *Oh et al.*,³ the strain-field curve of our coarse-grain ceramic clearly shows hysteresis. Despite the fact that the permittivity peak of the fine-grain BTS-5 ceramic displays characteristic features of diffuse phase transition ferroelectrics, the hysteresis of the $S(E)$ -curve remains unaffected. This indicates that domain-switching governs the electromechanical large-field response in our samples BTS-5 irrespective of its grain size.

In conclusion, we have shown that BTS powder obtained from glycolate-precursors is basically applicable to sinter BTS-ceramic with modified microstructure and thus modified dielectric and electromechanical properties. Further efforts are required to find appropriate sintering-additives and -conditions, leading to optimised microstructure and performance of the ceramic for electromechanical applications.

Acknowledgment

The authors are indebted to Mr. M. Rössel who carried out the ESEM investigation. This study was financially supported by DFG (Schwerpunktprogramm 1136 "Substitutionseffekte in ionischen Festkörpern").

Table 1:

	Fine-grain BTS-5	Coarse-grain BTS-5
$-d_{31}'$ (pm/V)	10.63	26.58
$-d_{31}''$ (pm/V)	0.14	0.58
$s_{11}^{E'} \times 10^{-12}$ (Pa ⁻¹)	12.31	9.46
Q	77	138
$K' \times 10^{-4}$	225	740
$K'' \times 10^{-4}$	2.9	5.6

Fig. 1:

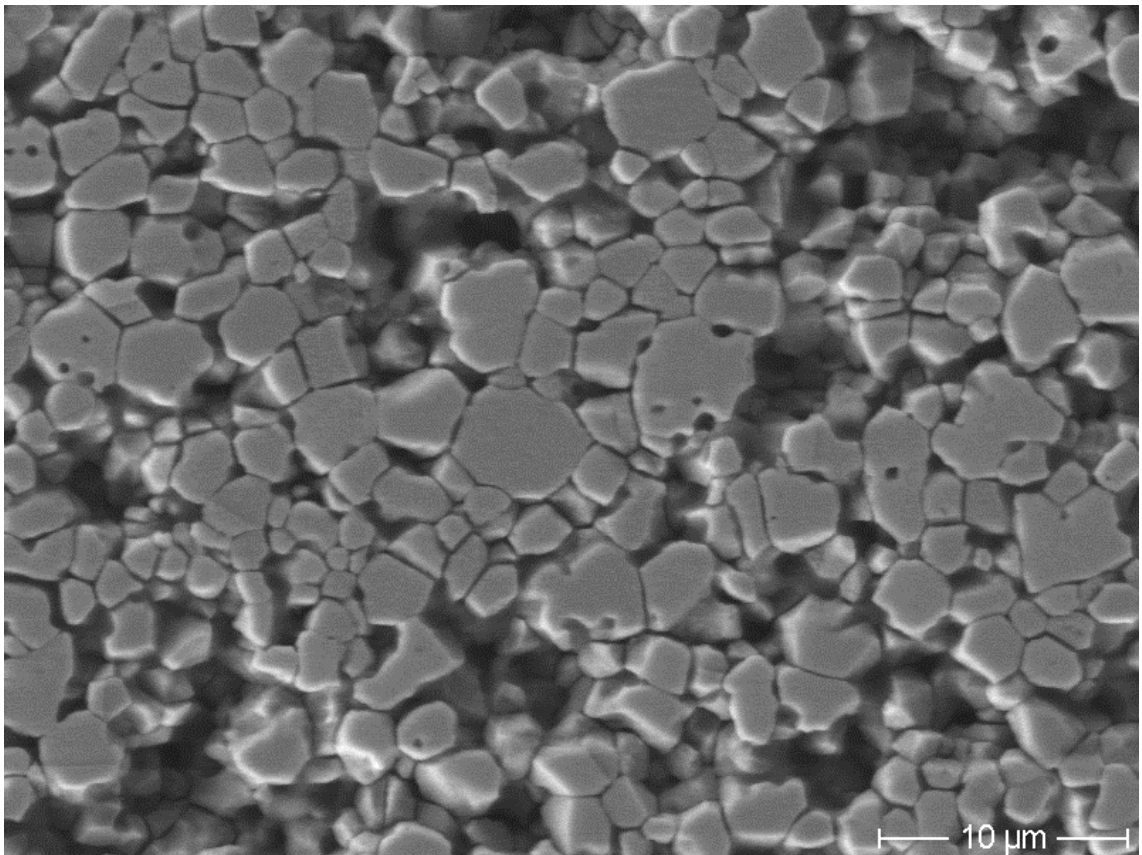


Fig. 2:

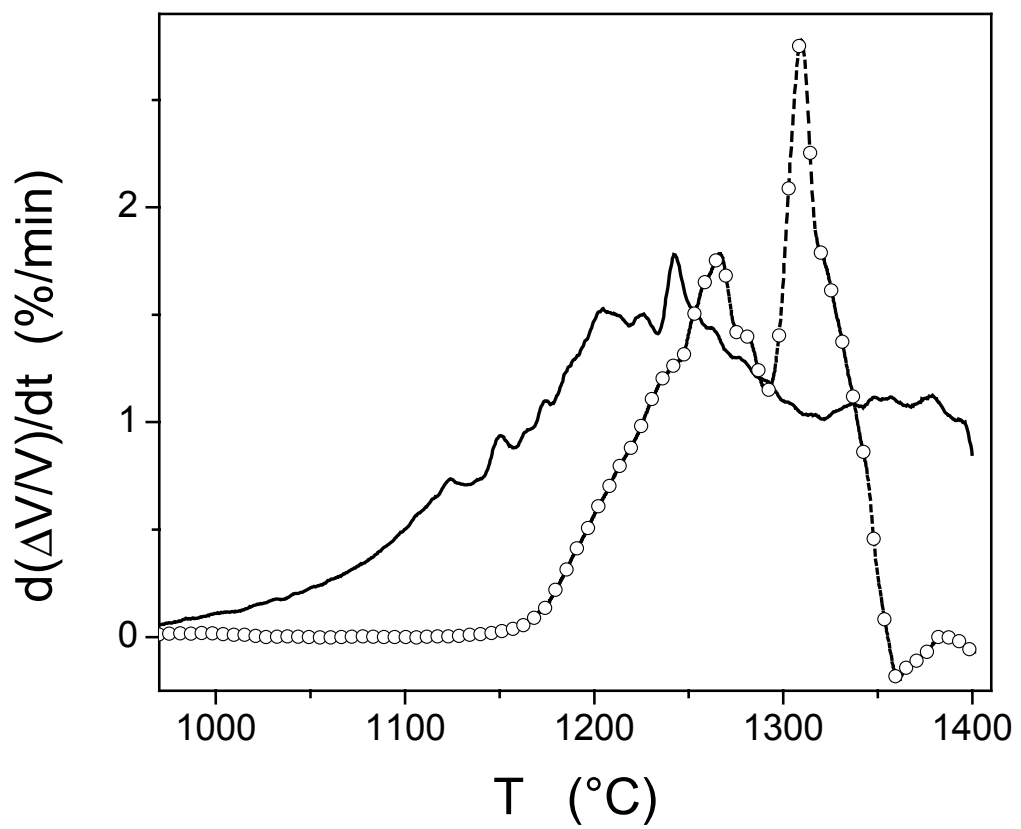


Fig. 3:

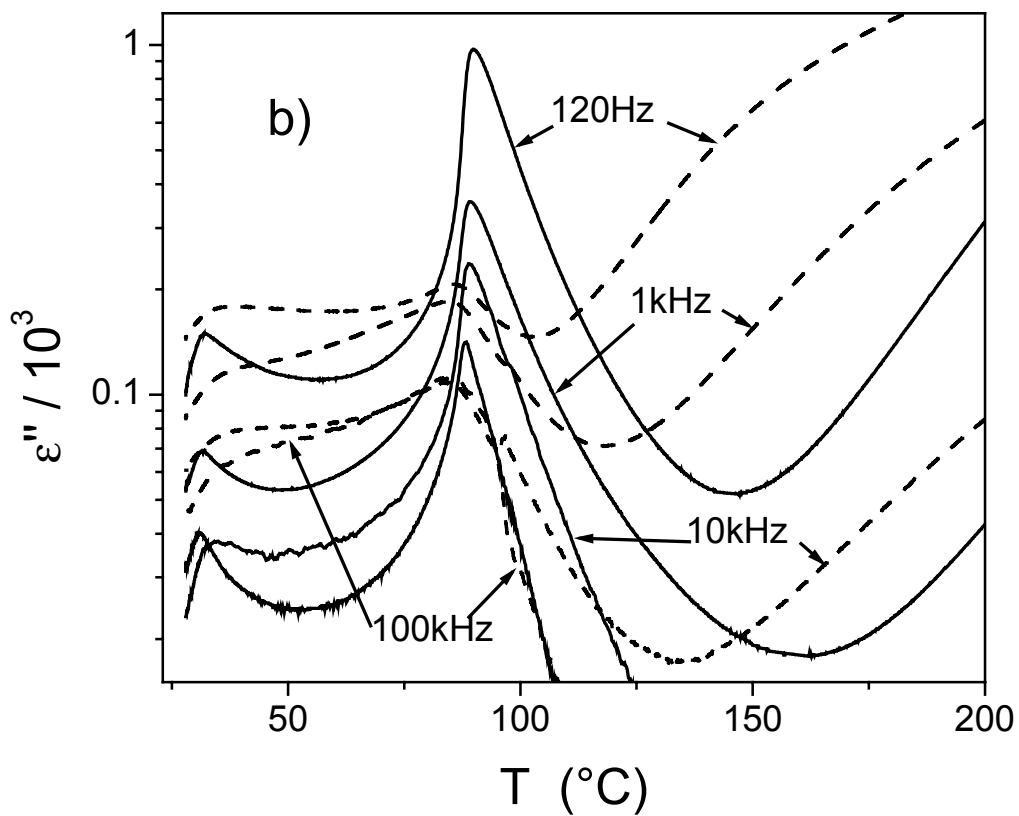
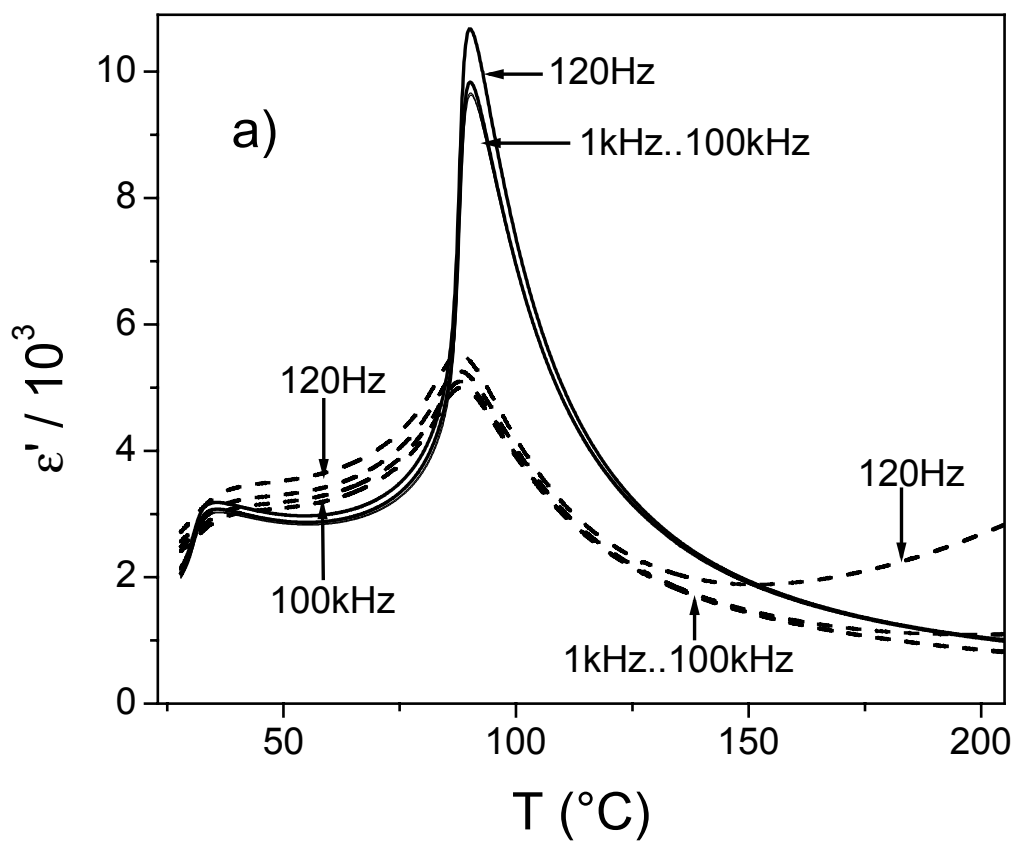


Fig. 4:

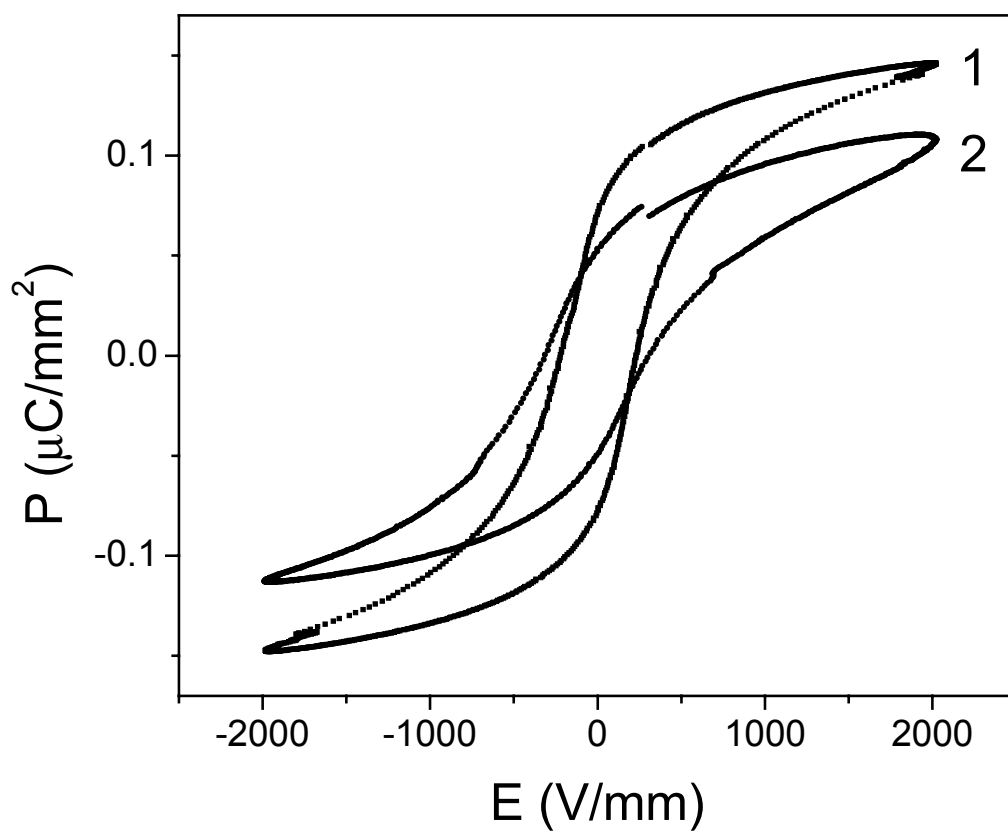
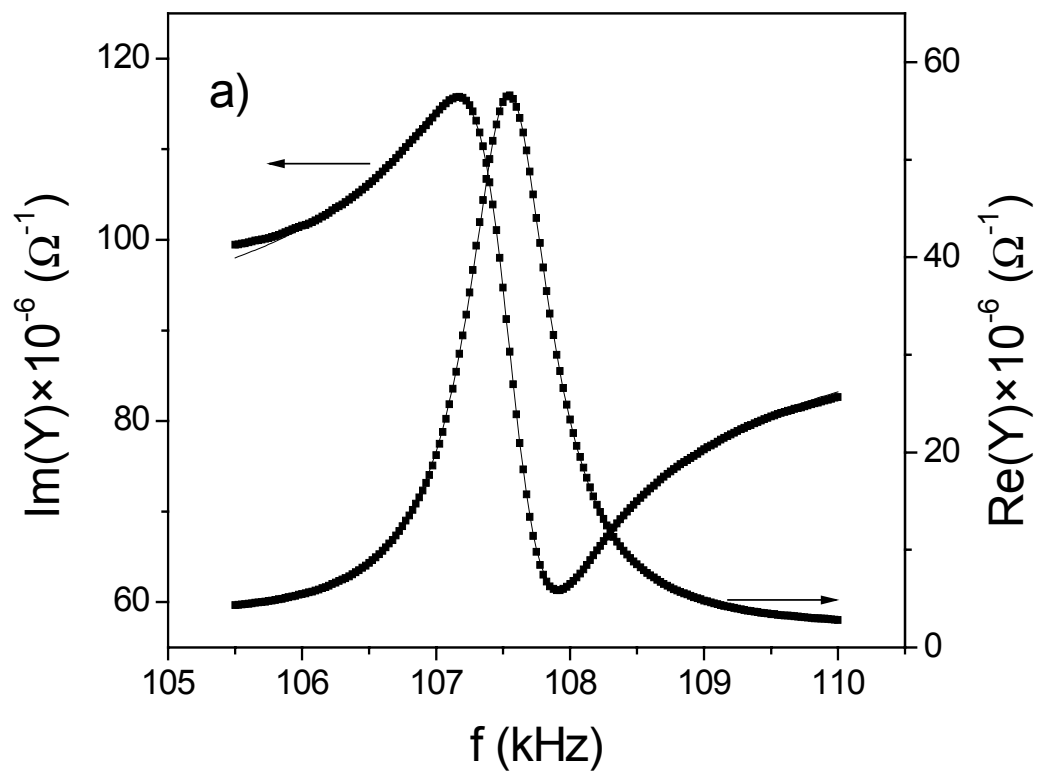


Fig. 5:



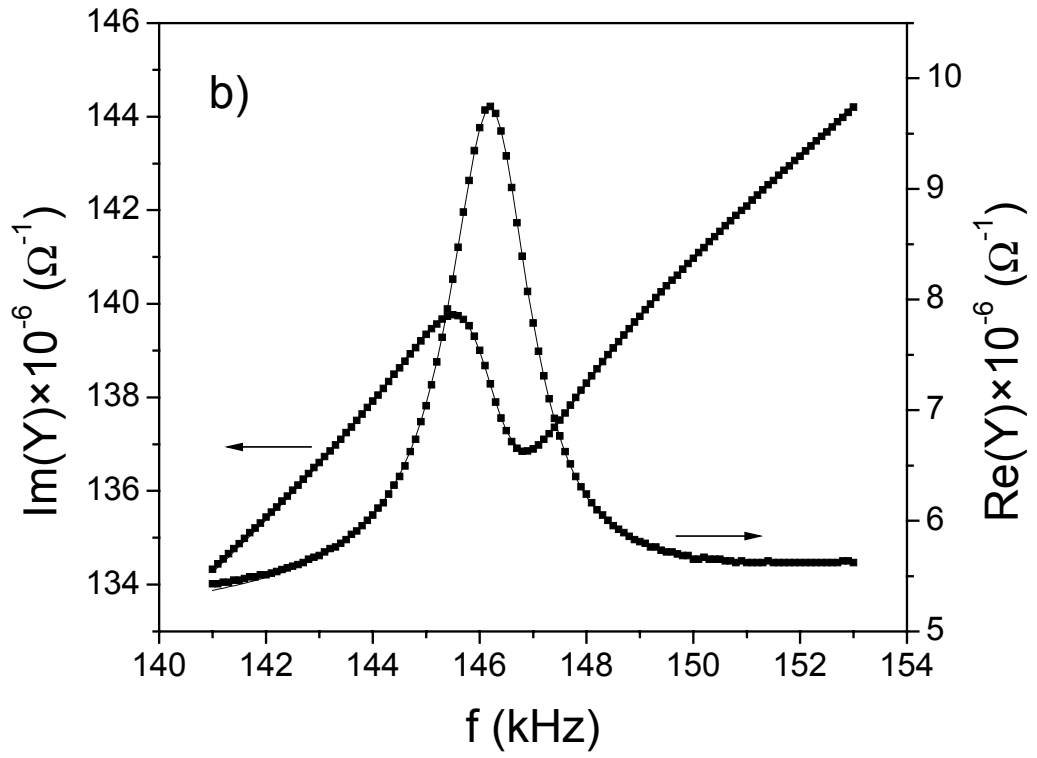
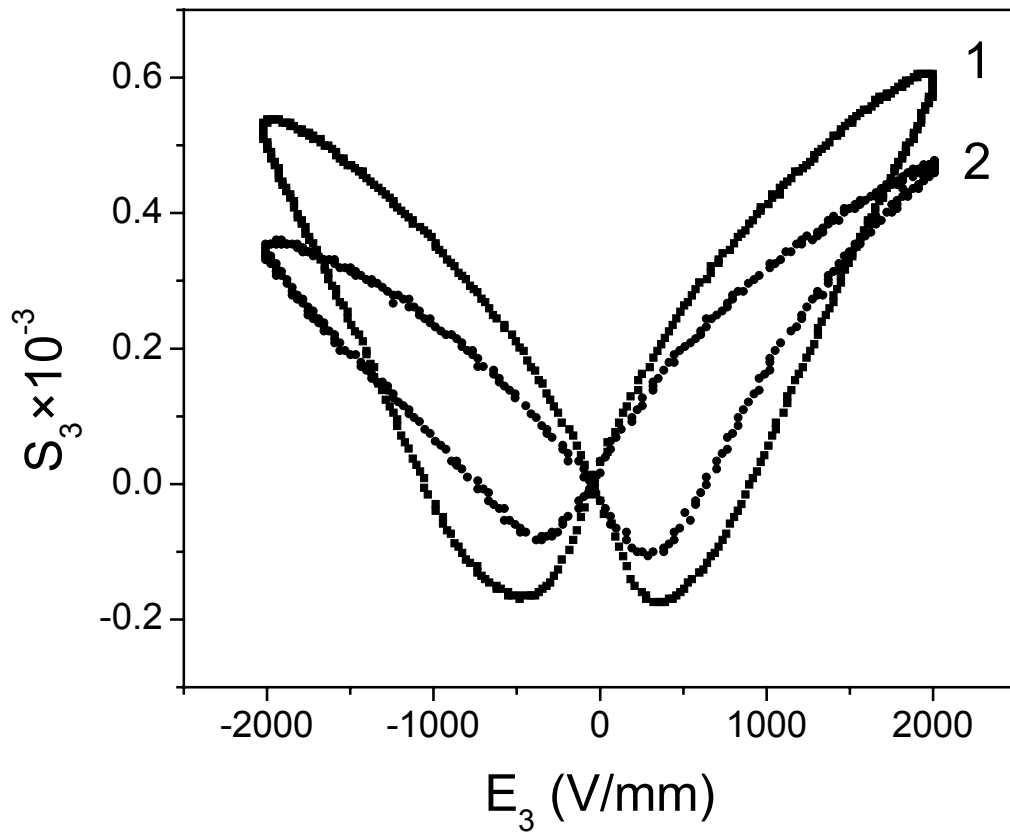


Fig. 6:



Captions

Fig.1: ESEM image showing the microstructure of the fine-grain BTS-5 ceramic.

Fig.2: Densification rate observed during sintering (heating rate 10K/min) of the mixed oxide powder (open symbols connected with dashed line) and of the glycolate precursor powder (full line).

Fig.3: Temperature dependence of a) the real part and b) the imaginary part of the permittivity, measured upon cooling of the coarse-grain (full line) and fine-grain (dash line) ceramic.

Fig.4: Ferroelectric hysteresis loop ($f=200\text{Hz}$) measured at room temperature for (1) coarse-grain and (2) fine-grain BTS-5.

Fig.5: Resonance spectra measured for a) coarse-grain and b) fine-grain BTS-5.

Fig.6 Strain-field dependence ($f=10\text{Hz}$) measured at room temperature for (1) coarse-grain and (2) fine-grain BTS-5.

References

- ¹ Smolensky, G. A., Physical Phenomena in Ferroelectrics with Diffused Phase Transition. *J. Phys. Soc. Jpn.*, 1970, **28**, 26.
- ² Yasuda, N., Ohwa, H. and Asano, S., Dielectric Properties and Phase Transitions of Ba(Ti_{1-x}Sn_x)O₃ Solid Solution. *Jpn. J. Appl. Phys.*, 1996, **35**, 5099-5103.
- ³ Oh, K., Uchino, K. and Cross, L. E., Optical Study of Domains in Ba(Ti,Sn)O₃ Ceramics. *J. Am. Ceram. Soc.*, 1994, **77**, 2809-2816.
- ⁴ Mueller, V., Beige, H. and Abicht, H.-P., Non-Debye dielectric dispersion of barium titanate stannate in the relaxor and diffuse phase-transition state. *Appl. Phys. Lett.*, 2004, in press.
- ⁵ v. Cieminski, J., Langhammer, H. T. and Abicht, H.-P., Peculiar Electromechanical Properties of Some Ba(Ti,Sn)O₃ Ceramics. *phys. stat. sol. (a)*, 1990, **120**, 285-293.
- ⁶ Mueller, V., Kouvatov, A., Steinhausen, R., Beige, H. and Abicht, H.-P., Ferroelectric and relaxor-like electromechanical strain in BaTi_{1-x}Sn_xO₃ ceramics. to appear in *Ferroelectrics*.
- ⁷ Simon, A., Ravez, J. and Maglione, M., The crossover from a ferroelectric to a relaxor state in lead-free solid solutions. *J. Phys.: Condens. Matter*, 2004, **16**, 963-970.
- ⁸ Hackenberger, W. S., Pan, M. J., Vedula, V., Pertsch, P., Cao, W., Randall, C. A. and Shrout, T. R., Smart structures and materials. In *Smart Materials Technologies*, ed. M. Wuttig. Proc. SPIE **3324**, 1998, 28-36.
- ⁹ Hennings, D., Barium Titanate Based Ceramic Materials for Dielectric Use. *Int. J. High Technology Ceramics*, 1987, **3**, 91-111.
- ¹⁰ Polotai, A. V., Ragulya, A. V. and Randall, C. A., Preparation and size effect in pure nanocrystalline barium titanate ceramics. *Ferroelectrics*, 2003, **288**, 93-102.
- ¹¹ Demartin, M. and Damjanovic, D., Dependence of the direct piezoelectric effect in coarse and fine grain barium titanate ceramics on dynamic and static pressure. *Appl. Phys. Lett.*,

1996, **68**, 3046-3048.

¹² Arlt, G., Hennings, D. and de With, G., Dielectric properties of fine-grained barium titanate ceramics. *J. Appl. Phys.*, 1985, **58**, 1619-1625.

¹³ Park, Y., Lee, W. J. and Kim, H. G., Particle-size-induced diffuse phase transition in the fine-particle barium titanate porcelains. *J. Phys.: Condens. Matter*, 1997, **9**, 9445-9456.

¹⁴ Cerda, J., Arbiol, J., Diaz, R., Dezanneau, G. and Morante, J. R., Synthesis of perovskite-type BaSnO₃ particles obtained by a new simple wet chemical route based on a sol-gel process. *Mater. Lett.*, 2002, **56**, 131-136.

¹⁵ Udawatte, C. P., Kakihana, M. and Yoshimura, M., Preparation of pure perovskite-type BaSnO₃ powders by the polymerized complex method at reduced temperature. *Solid State Ionics*, 1998, **108**, 23-30.

¹⁶ Leoni, M., Viviani, M., Nanni, P. and Buscaglia, V., Low-temperature aqueous synthesis (LTAS) of ceramic powders with perovskite structure. *J. Mater. Sci. Lett.*, 1996, **15**, 1302-1304.

¹⁷ Day, V. W., Eberspacher, T. A., Frey, M. H., Klemperer, W. G., Liang, S. and D. A. Payne, Barium titanium glycolate: A new barium titanate powder precursor. *Chem. Mater.*, 1996, **8**, 330.

¹⁸ Jäger, L., Lorenz, V., Müller, T., Abicht, H.-P., Rössel, M. and Görls, H., unpublished.

¹⁹ Jäger, L., Lorenz, V., Müller, T., Abicht, H.-P., Rössel, M. and Görls, H., Barium Stannate Powders from Hydrothermal Synthesis and by Thermolysis of Barium-Tin(IV)-Glycolates. Synthesis and Structure of [Ba(C₂H₆O₂)₄][Sn(C₂H₄O₂)₃] and [Ba(C₂H₆O₂)₂][Sn(C₂H₄O₂)₃]·CH₃OH. *Z. Anorg. Allg. Chem.*, 2004, **630**, 189-195.

²⁰ Smit, J. G., Iterative Method for Accurate Determination of the Real and Imaginary Parts of the Material Coefficients of Piezoelectric Ceramics. *IEEE Trans. Son. Ultrason.*, 1976, **SU-**

23, 393-402.

²¹ Sorge, G., Hauke, T. and Klee, M., Electromechanical properties of thin ferroelectric $\text{PbZr}_{0.53}\text{Ti}_{0.47}\text{O}_3$ -layers. *Ferroelectrics* 1995, **163**, 77-88.

²² Abicht, H.-P., Völtzke, D., Schneider, R. and Woltersdorf, J., The influence of the milling liquid on the properties of barium titanate powders and ceramics. *J. Mat. Chem.*, 1997, **7**, 487-492.

²³ Frey, M. H., Payne, D. A., Grain-size effect on structure and phase transformations for barium titanate. *Phys. Rev. B*, 1996, **54**, 3158-3168.

²⁴ Jaffe, B., Cook, J. and Jaffe, H., *Piezoelectric Ceramics*, (Academic, London 1971).

²⁵ Tsurumi, T., Kil, Y.-B., Nagatoh, K., Kakemoto, H. and Wada, S., Intrinsic Elastic, Dielectric, and Piezoelectric Losses in Lead Zirconate Titanate Ceramics Determined by an Impedance-Fitting Method. *J. Am. Ceram. Soc.*, 2002, **85**, 1993-1996.